Mathematical modelling of norovirus transmission incorporating human and environmental factors with evaluation of screening and supportive treatment

K.A. Tijani[*], **A. Abokwara**[† ‡], **L. Mbaskabkwe**[§], and **A.E. Salih**[¶]

Abstract

Norovirus is a highly contagious viral pathogen that causes acute gastroenteritis, resulting in vomiting and diarrhoea. It accounts for approximately 200,000 deaths each year, including 50,000 child fatalities globally, highlighting its substantial impact on public health. This study investigated the transmission dynamics of norovirus using a mathematical modelling approach. The basic reproduction number is computed and used to establish the stability of the disease-free equilibrium (DFE) and the endemic equilibrium (EE), such that the DFE is locally and globally asymptotically stable when $R_0 < 1$, while the EE is locally and globally asymptotically stable whenever $R_0 > 1$. With the aid of Partial Rank Correlation Coefficients (PRCCs) and Latin Hypercube Sampling (LHS), a global sensitivity analysis identifies pathogen decay due to disinfection and proper sanitation (μ_a), recovery rate resulting from screening and supportive treatment (γ), shedding rate (π), and effective environment-to-human transmission rate (β_{EH}) as the most significant parameters influencing disease spread. Findings from numerical simulations show that, to control this disease in society, intensive screening, supportive treatment, hygiene practices, disinfection, and proper sanitation should be implemented.

Keywords: global sensitivity analysis; mathematical model; reinfection; stability analysis; screening and supportive treatment

1 Introduction

Norovirus, also called the vomiting bug or stomach flu [1], is a highly contagious viral infection that causes acute gastroenteritis, resulting in vomiting and diarrhoea [1, 2]. It spreads easily and quickly through particles from feces or oral mucus [3], by having direct contact with infected individuals, consuming food or liquids contaminated with the virus, or touching contaminated objects or surfaces and then placing unwashed hands in the mouth [4]. Norovirus has an incubation period ranging from 12 to 48 hours [5]. Symptoms include nausea, diarrhoea, abdominal pain, fever, headache, and stomach pain, among others, and the infection can be fatal if left untreated [1]. Norovirus symptoms are typically self-limiting, with recovery occurring within 1 to 3 days in most cases [6].

Norovirus can infect individuals of all ages, and anyone may be affected during outbreaks. Meanwhile, people at the extremes of age and immunocompromised individuals face the greatest risk of adverse outcomes, while older adults are at increased risk of fatal outcomes even though, being infected with a norovirus is also determined by a gene. Globally, an estimated 685 million cases of norovirus occur annually, including 200 million among children under the age of five. The virus causes about 200,000 deaths each year, of which 50,000 are child deaths [2, 4].

[*]Department of Mathematics, Joseph Sarwuan Tarka University, Makurdi, Nigeria; Email:kazeemtijani1987@yahoo.com
[†]Corresponding Author; E-mail: agathamicheal@gmail.com
[‡]Department of Mathematics, Joseph Sarwuan Tarka University, Makurdi, Nigeria
[§]Department of Mathematics, Federal University of Education, Zaria, Nigeria; Email:lukambaskabkwe@gmail.com
[¶]Department of Mathematics, Joseph Sarwuan Tarka University, Makurdi, Nigeria; Email: salih.abdulwahab@uam.edu.ng

Currently, no vaccine is available for the prevention of norovirus, although efforts are underway to develop one [3]. Preventive measures include consistent hygiene practices such as handwashing with soap, use of gloves and face masks, proper environmental sanitation with adequate ventilation, and disinfection of contaminated areas [6]. Norovirus has no specific treatment, with management relying on supportive care and fluid intake to prevent dehydration, and reinfection remains possible even after recovery [7] .

Mathematical modelling involves representing real-world problems in mathematical terms, typically through equations, which are then used to enhance understanding, reveal new features, and develop solutions [8] . The concept of mathematical modelling of infectious diseases is an essential tool for analysing their dynamic nature, and it helps in developing and forecasting appropriate control strategies [9, 10]. Several authors have employed mathematical modelling to propose solutions to infectious diseases, such as Madubueze *et al.* [11] on schistosomiasis, Madubueze *et al.* [12] on the dynamics of diphtheria, Tijani *et al.* [13] on typhoid fever, Abokwara and Madubueze [14] on filariasis, and Sayooj *et al.* [15] on dengue fever, among others. Some authors, [16, 17, 18, 19, 20, 21, 22, 23, 24] have also used this concept of mathematical modelling in investigating the dynamics of norovirus disease.

Gaythorpe *et al.*, [17] considered susceptible, $S(t)$, exposed, $E(t)$, infected, $I(t)$, and recovered, $R(t)$, deterministic model with the incorporation of individuals protected by maternal antibodies, $M(t)$. They replicated this disease transmission model for individuals who were vaccinated but did not belong to the maternal protection class. Their findings indicate that the implementation of a vaccine could reduce the incidence of norovirus to 70.5%. However, they did not consider virus concentration in their work. In addition, they did not conduct major qualitative analyses, such as local and global stability of the disease-free equilibrium (DFE) and endemic equilibrium (EE) states. Global sensitivity analysis was also not taken into account. Raezal *et al.*, [22] formulated a deterministic model comprising the susceptible class $H(t)$, Vaccinated individuals $V(t)$, Asymptomatic or exposed individuals, $U(t)$, Symptomatic or infectious individuals, $A(t)$, and the recovered class, $C(t)$, using fractional order method.The outcome of their findings provides valuable insight into the dynamics of the disease; however, they failed to incorporate the virus concentration class [1], which is of critical importance in understanding disease dynamics. They did not examine the global stability of the disease-free equilibrium (DFE), nor the local and global stability of the endemic equilibrium (EE). In addition, they failed to account for the potential reinfection of recovered individuals, since no permanent immunity follows recovery [7]. Saleem *et al.*, [23] also constructed an SEIR model using the fractional-order technique, and their findings indicate that fractional-order models perform better than classical integer-order models. However, they did not include protected or virus concentration classes in their model. In addition, they failed to account for the reinfection of recovered individuals, as no permanent immunity follows recovery [7]. Their study did not address the local and global stability of the endemic equilibrium (EE), nor did it incorporate global sensitivity analysis. Gogovi *et al.,* [18] established a compartmental model comprising susceptible class $S(t)$, asymptomatic infected individuals, $A(t)$, symptomatic individuals, $I(t)$, and the virus concentration class, $R(t)$ to examine the dynamics of the norovirus. Their findings highlight the importance of environmental interventions, such as environmental decontamination. However, they did not include the exposed class, which reflects the impact of the incubation period on disease dynamics, nor did they consider the protected and recovered classes. Furthermore, they failed to account for the potential reinfection of recovered individuals, since no permanent immunity follows recovery, as stated by [2]. According to Gaythorpe *et al.* [16], an SEIR model was developed to study norovirus dynamics, revealing substantial variability in parameter estimates such as the reproduction number. The model excluded virus concentration in the environment and the possibility of reinfection among recovered individuals. While the study relied on quantitative analyses, it neglected qualitative aspects, including the stability of DFE and EE states, and omitted global sensitivity analysis. Song *et al.* [20] developed a stochastic SIRWF model that integrates susceptible, infected, recovered, water contamination, and food contamination classes. While their findings demonstrate a robust framework for complex biological and epidemiological phenomena, the model excluded exposed and protected classes, overlooked reinfection among recovered individuals due to the absence of permanent immunity, and did

not incorporate global sensitivity analysis. In the work of Cui *et al.* [21], they formulated fractal-fractal and stochastic models to investigate the dynamics of norovirus, incorporating the susceptible class vaccinated individuals, asymptomatic or exposed individuals, symptomatic or infectious individuals, and the recovered class. Their results provide a theoretical basis for understanding the dynamics of this globally contagious disease. However, they did not account for virus concentration in the environment, nor did they examine the possibility of reinfection among the recovered population, as the disease does not confer permanent immunity after recovery. Furthermore, they did not include global sensitivity analysis in their study. In their study, Towers *et al.* [24] established a deterministic SEIR model incorporating virus concentration in the environment to examine the dynamics of norovirus on a cruise ship. Their findings indicate that environmental transmission can lead to sustained outbreaks aboard cruise ships when strict sanitation practices are neglected, while direct transmission remains dominant. They further concluded that promoting proper handwashing practices should be strongly encouraged. While Lopman *et al.*, [19] formulated a reinfection SEIAR mathematical model. Their findings reveal that among older children and adults, the incidence of the disease would increase from 6% to 16%. Their results also highlight the limitations of case-control studies for pathogens with suboptimal diagnostic specificity.

Although previous studies have made substantial contributions to norovirus control, several critical gaps persist. To address these, this work develops a nonlinear deterministic model incorporating susceptible $(S_h(t))$, protected $(P_h(t))$, latent $(L_h(t))$, infected $(I_h(t))$, and recovered $(R_h(t))$ human populations, together with environmental pathogen concentration $(V_c(t))$. The protected population, $P_h(t)$ comprises individuals who follow safety precautions, as well as members of the recovered population adhering to safety measures [25]. The model aims to capture both direct and indirect transmission pathways and the potential for reinfection, as highlighted by [2, 7], thereby guiding the design of effective and sustainable interventions.

The remainder of the paper is organized as follows: Section 2 presents the model formulation, while Section 3 provides the qualitative analysis. Section 4 discusses the numerical simulations, along with the results. Finally, Section 5 concludes the paper.

2 Model formulation

In this paper, a nonlinear mathematical model is formulated to investigate the dynamics of norovirus, considering both direct and indirect transmission modes. The human population is divided into five compartments at time t: susceptible humans $S_h(t)$, protected humans $P_h(t)$, latent or pre-infectious humans $L_h(t)$, infected humans $I_h(t)$, and recovered humans $R_h(t)$, where

$$N_h(t) = S_h(t) + P_h(t) + L_h(t) + I_h(t) + R_h(t). \tag{1}$$

The model also considers the norovirus pathogen concentration in the environment $V_c(t)$. The model assumes a homogeneous population at all times [1], where susceptible individuals may be protected through preventive measures [3], are at risk of infection via direct human-to-human or indirect environmental transmission [2], may die from the disease [4], and can be reinfected after recovery [1].

Births and immigration augment the susceptible population, $S_h(t)$ at rate Λ, while a proportion, ρ of recovered individuals re-enter susceptibility at rate θ following loss of immunity [7]. Individuals in the susceptible compartment, $S_h(t)$ progress to the protected compartment $P_h(t)$ at rate α due to adherence to effective preventive measures [3, 6]. In addition, the protected population $P_h(t)$ increases by a proportion $(1-\rho)$ at rate θ through the transition of recovered individuals $R_h(t)$ who adopt preventive measures. The susceptible population can acquire the infection at rate λ, transitioning into the pre-infectious or latent state $L_h(t)$. The force of infection is defined by the equation $\lambda = \left[\beta_{HH} I_h + \frac{\beta_{EH} V_c}{K+V_c}\right]$. In this equation, β_{HH} denotes the effective transmission rate from human to human, while β_{EH} represents the effective transmission rate from the environment to humans [2]. The parameter, K corresponds to the environmental carrying capacity.

Individuals in the latent compartment $L_h(t)$ leave this class at rate σ and subsequently progress to the infected class, $I_h(t)$ following the incubation period [5]. The population of individuals in the infected class, denoted as, $I_h(t)$ decreases due to disease-induced mortality at rate δ. In addition, infected individuals progress to the recovered class $R_h(t)$ at rate γ [1]. Additionally, μ represents the natural death rate of the human population. The concentration of the norovirus pathogens in the environment increases due to shedding from both the infected class, I_h, at rates π [3, 4]. Furthermore, the concentration of pathogens decreases due to the natural and artificial decay rates, μ_v and μ_a [2].

A graphical representation of the model formulation is shown in Figure 1, while the state variables and parameter descriptions are detailed in Table 1 and 2, respectively. The following system of non-

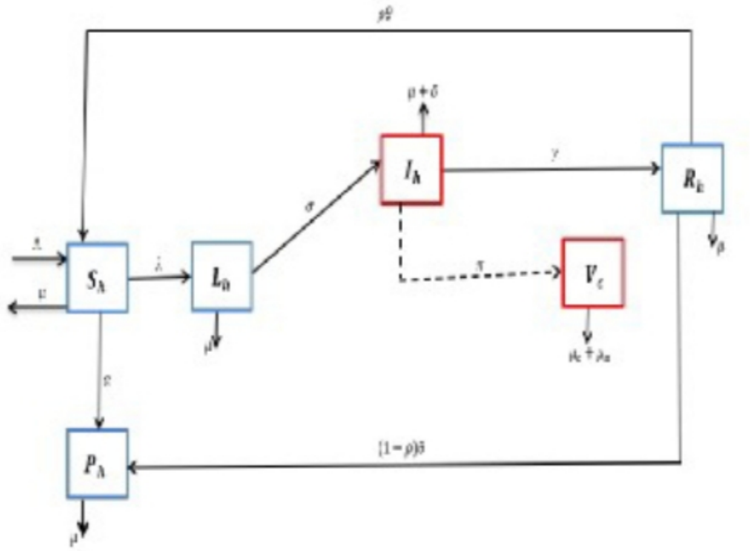

Figure 1: Schematic diagram of the norovirus disease

Table 1: State Variables of the model

Parameter	Symbol	Unit
Susceptible human population per time, t	$S_h(t)$	humans
Protected human population per time, t	$P_h(t)$	humans
Latent(pre-infectious) human population per time, t	$L_h(t)$	humans
Infected human population per time, t	$I_h(t)$	humans
Recovered human population per time, t	$R_h(t)$	humans
Norovirus pathogen concentration in the environment per time, t	$V_c(t)$	pathogens

linear differential equations is formulated based on the assumptions of the model, the parameters in Table 1 and Table 2, respectively, while the flow diagram is shown in Figure 1 with the corresponding

system of equations in (2):

$$\left.\begin{aligned}
\frac{dS_h}{dt} &= \Lambda - \lambda S_h + \rho\theta R_h - (\alpha+\mu)S_h,\\
\frac{dP_h}{dt} &= \alpha S_h + (1-\rho)\theta R_h - \mu P_h,\\
\frac{dL_h}{dt} &= \lambda S_h - (\sigma+\mu)L_h,\\
\frac{dI_h}{dt} &= \sigma L_h - (\mu+\gamma+\delta)I_h,\\
\frac{dR_h}{dt} &= \gamma I_h - (\theta+\mu)R_h,\\
\frac{dV_c}{dt} &= \pi I_h - (\mu_v+\mu_a)V_c,
\end{aligned}\right\} \tag{2}$$

with non-negative initial conditions, $S_h(0) > 0$, $P_h(0) > 0$, $L_h(0) > 0$, $I_h(0) > 0$, $R_h(0) > 0$, $V_c(0) > 0$ and $\lambda = \left[\beta_{HH} I_h + \frac{\beta_{EH} V_c}{K+V_c}\right]$. The model parameters are assumed to be non-negative.

Table 2: Values of parameters used in simulation.

Parameter	Symbol	Value/Range	Source
Human recruitment rate	Λ	400	Estimate
Human-to-human effective transmission rate	β_{HH}	0.0178	[26]
Environment-to-human effective transmission rate	β_{EH}	0.0122(0.01-0.03)	[27]
Progress rate from L_h to I_h after latent period	σ	0.5	[5, 6]
Progress rate from S_h to P_h	α	0.0001	[6]
Human natural death rate	μ	0.0004	[28]
Disease induced death rate for human	δ	0.33	[29]
Recovery rate from I_h to R_h due to screening and supportive treatment	γ	0.8378	[17]
Progress rate from R_h to S_h and P_h due to loss of immunity and adherence to protective measures respectively	θ	0.00034	[17]
Shedding rate from I_h to V_c	π	0.05	Assume
Proportion of recovered individuals that became susceptible after loss of immunity	ρ	0.85	[1]
Natural pathogen decay rate	μ_v	0.004(0.004-0.07)	[30]
Pathogen decay rate due to artificial means like disinfection and proper sanitation	μ_a	0.09	[18]
Carrying capacity	K	500000	[31]

3 Analysis of the model

3.1 Positivity of the state variables

To establish the solution's positivity, we present and demonstrate the following theorem.

Theorem 3.1. *For any non-negative initial conditions, the solutions* $\Big(S_h(t), P_h(t), L_h(t), I_h(t), R_h(t), V_c(t)\Big)$ *of system* (2) *remain non-negative for all* $t > 0$.

Proof. We demonstrate that the solution $S_h(t)$ remains non-negative. Suppose that at time t_1, $S_h'(t_1) < 0$, $P_h(t_1) > 0$, $L_h(t_1) > 0$, $I_h(t_1) > 0$, $R_h(t_1) > 0$, $V_c(t_1) > 0$. From the first equation of system (2),

$$S_h'(t_1) = \Lambda_h - \left[\beta_{HH} I_h + \frac{\beta_{EH} V_c}{K+V_c}\right](t_1) S_h(t_1) + \rho\theta R_h(t_1) - (\alpha+\mu)S_h(t_1) = \Lambda_h + \rho\theta R_h(t_1) > 0,$$

This contradicts the assumption that $S_h'(t_1) < 0$. Therefore, $S_h(t) > 0$ for $t > 0$.

For $P_h(t)$, assume there exist a time, t_2, $t_1 \neq t_2$ such that $P_h(t_2) = 0$, with $P_h'(t_2) < 0$ and all other variables being non negative at $t \neq t_2$, then from the second equation of model (2),

$$P_h'(t_2) = \alpha S_h(t_2) + (1-\rho)\theta R_h(t_2) - \mu P_h = \alpha S_h(t_2) + (1-\rho)\theta R_h(t_2) > 0.$$

This contradicts the assumption that $P_h'(t_2) < 0$. Hence, $P_h(t) \geq 0$ for $t > 0$.

For $L_h(t)$, assume there exist a time, t_3 such that $L_h(t_3) = 0$, with $L_h'(t_3) < 0$ with all other variables being non negative at $t = t_3$, then from the third equation of model (2),

$$L_h'(t_3) = \left[\beta_{HH} + \frac{\beta_{EH} V_c}{K + V_c}\right](t_3) S_h(t_3) - (\sigma + \mu) L_h = \left[\beta_{HH} + \frac{\beta_{EH} V_c}{K + V_c}\right](t_3) S_h(t_3) > 0.$$

This contradicts the assumption that $L_h'(t_3) < 0$. Hence, $L_h(t) \geq 0$ for $t > 0$.

In the same way, it can be shown for $I_h(t), R_h(t)$, and $V_c(t)$ for $t > 0$. Therefore, we can conclude that the solutions $(S_h(t), P_h(t), L_h(t), I_h(t), R_h(t), V_c(t))$ of system (2) are non- negative for $t > 0$. The result confirms the model's validity and biological relevance, as negative population sizes are not physically possible.

3.2 Invariant region

For all time $t \geqslant 0$, the parameters of the model are biologically meaningful, as they are taken to be non-negative along with the initial conditions. Consequently, the analysis of model (2) will be carried out within an appropriate feasible region, defined as follows At any time t, the total human population is denoted by $N_h(t)$ is

$$N_h(t) = S_h(t) + P_h(t) + L_h(t) + I_h(t) + R_h(t), \tag{3}$$

and $V_c(t)$ is the virus population. with initial conditions $N_h(0)$= N_{h0}, and $V_c(0) = V_{c0}$ respectively. We state the following lemma.

Lemma 3.2. *Every feasible solution remains uniformly bounded in a suitable subset of the domain*

$$Q = Q_h \times Q_c,$$

where

$$Q_h = \left\{(S_h, P_h, L_h, I_h, R_h) \in \mathbb{R}_+^5 : N_h(t) \leq \frac{\Lambda}{\mu}\right\},$$

and

$$Q_c = \left\{V_c \in \mathbb{R}_+ : 0 < V_c(t) \leq \frac{\pi\Lambda}{\mu(\mu_v + \mu_a)}\right\}$$

are subsets for human and virus populations, respectively.

Proof. Considering the human population,

$$\frac{dN_h}{dt} = \Lambda - \mu N_h - \delta I_h < \Lambda_h - \mu N_h. \tag{4}$$

By applying the Birkhoff and Rota theorem [32] on differential inequalities and integrating both sides of equation (4), we obtain the following result.

$$\int \frac{dN_h}{\Lambda - \mu N_h} \leq \int dt.$$

This implies that

$$\Lambda - \mu N_h \geq W_h \exp(-\mu t) \tag{5}$$

with W_h as a positive constant. Moreover, by substituting the initial conditions into equation (5), we obtain

$$\Lambda - \mu N_h \geq [\Lambda_h - \mu N_h(0)]\, e^{-\mu_h t}$$

which simplifies to

$$N_h \leq \frac{\Lambda}{\mu} - \left\{\frac{\Lambda - \mu N_h(0)}{\mu}\right\} e^{-\mu t}. \tag{6}$$

As $t \longrightarrow \infty$ in equation (6), the human population size, N_h approaches $\frac{\Lambda}{\mu}$. Therefore, all feasible regions of the human populations, S_h, P_h, L_h, I_h, and R_h enter the region

$$Q_h = \left\{(S_h, P_h, L_h, I_h, R_h) \in \mathbb{R}_+^5 : N_h(t) \leq \frac{\Lambda}{\mu}\right\}.$$

For the virus population, we have from the sixth equation in system (2) that

$$\frac{dV_c}{dt} = \pi I_h - (\mu_v + \mu_a)V_c$$

But, $I_h \leq N_h(t)$ and $I_h \leq N_h \leq \frac{\Lambda}{\mu}$, we have

$$\frac{dV_c}{dt} \leq \frac{\pi\Lambda}{\mu} - (\mu_v + \mu_a)V_c. \tag{7}$$

and Rota theorem [32] for differential inequalities and integrating equation (7), we arrive at the following.

$$\int \frac{dV_c}{\frac{\pi\Lambda}{\mu} - (\mu_v + \mu_a)V_c} \leq \int dt,$$

which implies that

$$-\frac{1}{(\mu_v + \mu_a)} \ln\left(\frac{\pi\Lambda}{\mu} - (\mu_v + \mu_a)V_c\right) \leq t + V_m \tag{8}$$

with V_m as the constant of integration. It follows from equation (8) that

$$\ln\left(\frac{\pi\Lambda}{\mu} - (\mu_v + \mu_a)V_c\right) \geq -(\mu_v + \mu_a)(t + V_m).$$

Therefore,

$$\frac{\pi\Lambda}{\mu} - (\mu_v + \mu_a)V_c \geq W_m e^{(-\mu_v + \mu_a)t}, \tag{9}$$

where W_m is a positive constant. Furthermore, applying the initial condition, $V_c(0) = V_{c0}$, to equation (9) yields

$$W_m \leq \frac{\pi\Lambda}{\mu} - (\mu_v + \mu_a)V_c(0). \tag{10}$$

Substituting equation (10) into equation (9) gives

$$V_c \leq \frac{\Lambda\pi}{\mu(\mu_v + \mu_a)} - \left[\frac{\pi\Lambda}{\mu(\mu_v + \mu_a)} - \frac{(\mu_v + \mu_a)V_c(0)}{\mu}\right] e^{-(\mu_v + \mu_a)t}. \tag{11}$$

As $t \longrightarrow \infty$ in equation (11), the population size, V_c, approaches

$$Q_c \leq \frac{\Lambda\pi}{\mu(\mu_v + \mu_a)}.$$

Hence, the virus population will enter the positive invariant region, Q_c, where

$$Q_c = \left\{V_c \in \mathbb{R}_+ : 0 < V_c(t) \leq \frac{\Lambda\pi}{\mu(\mu_v + \mu_a)}\right\}.$$

This shows that any solution originating from initial conditions in $\mathbb{R}_+^6$ remains within this region for all $t > 0$,, confirming that it is a positively invariant set under the dynamics of model (2). Consequently, system (2) is both epidemiologically meaningful and mathematically well-posed within the interior of the domain Q. It is therefore appropriate to restrict our analysis to the behaviour of the flow generated by model (2) within this domain.

It follows that the model system (2) is epidemiologically well-posed and mathematically consistent, thereby serving as a robust framework for analysing and mitigating the transmission dynamics of norovirus.

3.3 Disease-free equilibrium and basic reproduction Number, R_0

The disease-free equilibrium of system (2), denoted by E_0, corresponds to the steady state in which norovirus is absent from the population. Solving equation (2) at the equilibrium state simultaneously gives the disease-free equilibrium (DFE)

$$E_0 = \left(S_h^0, P_h^0, L_h^0, I_h^0, R_h^0, V_c^0\right) = \left(\frac{\Lambda}{(\alpha+\mu)}, \frac{\alpha\Lambda}{\mu(\alpha+\mu)}, 0, 0, 0, 0\right) \tag{12}$$

where

$$k_1 = (\alpha+\mu), \quad k_2 = (\sigma+\mu), \quad k_3 = (\mu+\gamma+\delta), \quad k_4 = (\theta+\mu), \quad k_5 = (\mu_v+\mu_a). \tag{13}$$

Then, considering the three infected compartments of the system of equations (2) and using the concept of Next-generation matrix approach as deployed by [12, 13, 33, 34], we have

$$F = \begin{pmatrix} 0 & \frac{\Lambda\beta_{HH}}{(\alpha+\mu)} & \frac{\Lambda\beta_{EH}}{K} \\ 0 & 0 & 0 \\ 0 & 0 & 0 \end{pmatrix} \text{ and } V = \begin{pmatrix} k_2 & 0 & 0 \\ -\sigma & k_3 & 0 \\ 0 & -\pi & k_5 \end{pmatrix}.$$

Solving this to obtain the spectral radius of FV^{-1}, we obtain the basic reproduction number, R_0, as follows;

$$\left.\begin{aligned} R_0 &= R_{HH} + R_{EH}, \\ R_0 &= \frac{\sigma\Lambda\beta_{HH}}{k_1k_2k_3} + \frac{\sigma\Lambda\pi\beta_{EH}}{Kk_1k_2k_3k_5}, \\ R_0 &= \frac{\sigma\Lambda\beta_{HH}}{(\alpha+\mu)(\sigma+\mu)(\mu+\gamma+\delta)} + \frac{\sigma\Lambda\pi\beta_{EH}}{K(\alpha+\mu)(\sigma+\mu)(\mu+\gamma+\delta)(\mu_v+\mu_a)}, \end{aligned}\right\} \tag{14}$$

where R_{HH} is the contribution of human-to-human in the spread of the human norovirus disease while R_{EH} is the contribution of the environment-to-human in the transmission dynamics of the disease.

3.3.1 Global stability of the disease-free equilibrium state

We state the following lemma.

Lemma 3.3. *The system of equations* (2) *exhibits a locally asymptotically stable disease-free equilibrium when* $R_0 \leq 1$, *whereas the equilibrium becomes unstable if* $R_0 > 1$.

The following theorem demonstrates the global stability of the disease-free equilibrium point, E_0.

Theorem 3.4. *The disease-free equilibrium of the system described by* (2) *is globally asymptotically stable when* $R_0 \leq 1$, *and loses stability when* $R_0 > 1$.

Proof. As noted in Castillo-Chavez *et al.* [35], assuming the disease-free equilibrium is locally asymptotically stable for $R_0 < 1$, two additional conditions must be met to ensure its global asymptotic stability. These conditions are outlined below:

i The function $F(X_1, 0)$ represents a globally asymptotically stable equilibrium for $\frac{dX_1}{dt}$.

ii Let $G(X_1, Y_1) = AY - G^*(X_1, Y_1)$, where $G(X_1, Y_1) \geq 0$ for all $X_1, Y_1 \in Q$. Here, $A = D_Y G(X^*, 0)$ denotes an $M-$matrix, and Q represents the biologically feasible region of the model.

To facilitate analysis, we introduce new variables and decompose the system (2) into subsystems. Let $X_1 = (S_h, P_h)$, representing the populations of susceptible and protected individuals. Additionally, define $Y_1 = (L_h, I_h, V_c)$ to denote the infected compartments, such that $R_h = 0$. The reformulated system is expressed as follows:

$$\left.\begin{aligned}\frac{dX_1}{dt} &= F(X_1, Y_1)\\ \frac{dY_1}{dt} &= G(X_1, Y_1)\end{aligned}\right\} where \quad X_1 \in \mathbb{R}^2_+, Y_1 \in \mathbb{R}^3_+.$$

Consequently, the two vector-valued functions are defined as follows.

$$\left.\begin{aligned}F(X_1, Y_1) = \Big(\Lambda - \left[\beta_{HH} I_h + \frac{\beta_{EH} V_c}{K + V_c}\right] S_h + \rho\theta R_h - (\alpha + \mu) S_h,\\ \alpha S_h + (1-\rho)\theta R_h - \mu P_h,\Big)^T\\ G(X_1, Y_1) = \Big(\left[\beta_{HH} I_h + \frac{\beta_{EH} V_c}{K + V_c}\right] S_h - (\sigma + \mu) L_h,\\ \sigma L_h - (\mu + \gamma + \delta) I_h,\\ \pi I_h - (\mu_v + \mu_a) V_c\Big)^T\end{aligned}\right\}$$

Here, T denotes the transpose. For convenience, we treat X_1 as equivalent to $(X_1, 0)$ and Y_1 with $(0, Y_1) \in \mathbb{R}^2_+ \times \mathbb{R}^3_+$. Hence the reduced system: $\frac{dX_1}{dt} = F(X_1, 0)$ is

$$\left.\begin{aligned}\frac{dS_h}{dt} &= \Lambda_h - (\alpha + \mu) S_h,\\ \frac{dP_h}{dt} &= \alpha S_h - \mu P_h.\end{aligned}\right\} \tag{15}$$

The Jacobian matrix corresponding to the subsystem (15) is expressed as

$J(x^*) = \begin{pmatrix} -(\alpha+\mu) & 0 \\ \alpha & -\mu \end{pmatrix}$,

which has negative eigenvalues $-\mu$ and $-(\alpha + \mu)$, and

$$X^* = (S_h^{**}, P_h^{**}) = \left(\frac{\Lambda}{\alpha + \mu}, \frac{\alpha\Lambda}{\mu(\alpha + \mu)}\right)$$

is a global asymptotically stable equilibrium point for the reduced system $\frac{dX_1}{dt}, F(X_1, 0)$. These asymptotic dynamics do not depend on the initial conditions within $\mathbb{R}^6_+$. Based on the framework established by Castillo-Chavez *et al.* [35], the fixed point X^* is a globally asymptotically stable equilibrium of the system (2), provided that $R_0 < 1$, ensuring local asymptotic stability, and the condition $\frac{dX_1}{dt} = F(X_1, 0)$ admits a globally asymptotically stable equilibrium at X^0.

Condition two specifies that $G(X_1, Y_1) = AY - G^*(X_1, Y_1)$, where $G(X_1, Y_1) \geq 0$ for $X_1, Y_1 \in Q$, and $A = D_Y G(X^*, 0)$ is an $M - matrix$. For

Clearly $G(X_1, Y_1)$ satisfies the condition that

$G(X_1, 0) = 0$ and $G(X_1, Y_1) = A^* Y_1 - G^*(X_1, Y_1), G^*(X_1, Y_1) \geq 0$, where

$$A^* = D_Y G(X_1, 0) = \begin{pmatrix} -k_2 & \beta_{HH} S_h^0 & \frac{\beta_{EH} S_h^0}{K} \\ \sigma & -k_3 & 0 \\ 0 & \pi & -k_5 \end{pmatrix}$$

and

$$G^*(X_1, Y_1) = \begin{pmatrix} \left[\beta_{HH} + \frac{\beta_{EH}}{K}\right](S_h^0 - S_h) \\ 0 \\ 0 \end{pmatrix}.$$

Since the human population assume a steady-state value, $\left[\beta_{HH} + \frac{\beta_{EH}}{K}\right](S_h^0 - S_h) \geq 0$, since $S_h^0 \geq S_h$. Therefore, the system is globally asymptotically stable, implying that the virus, infected individuals, and the disease ultimately vanish, regardless of the initial number of infected humans.

From an epidemiological standpoint, norovirus will be eliminated from the population in the absence of external interventions, provided that the conditions ensuring the stability of the disease-free equilibrium are sustained.

3.4 The endemic equilibrium state

The endemic equilibrium state, E^e, is a condition in which norovirus persists within the population over time. We now solve for the endemic equilibrium state in terms of the latent human class, $L_h(t)$. From equation (1), the total human population is given by the sum of all human compartments

$$N_h(t) = S_h(t) + P_h(t) + L_h(t) + I_h(t) + R_h(t).$$

Using the sum and difference rule of differentiation at equilibrium, we have

$$\frac{dN_h}{dt} = \frac{dS_h}{dt} + \frac{dP_h}{dt} + \frac{dL_h}{dt} + \frac{dI_h}{dt} + \frac{dR_h}{dt} = 0. \tag{16}$$

But,

$$N_h = \Lambda - \mu N_h - \delta I_h \implies N_h^e = \frac{\Lambda - \delta I_h^e}{\mu}. \tag{17}$$

Also, from equation (13), we have

$$\left.\begin{aligned} &I_h^e = \frac{\sigma L_h^e}{k_3},\ R_h^e = \frac{\gamma\sigma L_h^e}{k_3 k_4},\ \text{and } V_c^e = \frac{\pi\sigma L_h^e}{k_3 k_5}, \\ &\quad \text{and using the first and second equations of the model (2),} \\ &P_h^e = \frac{\alpha S_h^e k_3 k_4 + (1-\rho)\theta\gamma\sigma L_h^e}{\mu k_3 k_4}. \end{aligned}\right\} \tag{18}$$

Using equations (16), (17), (18) and substituting the second, third, fourth and fifth equations of the system (2) result in.

$$\frac{\Lambda k_3 - \delta\sigma L_h^e}{\mu k_3} = \Lambda + \frac{\rho\theta\gamma\sigma L_h^e}{k_3 k_4} - k_1 S_h^e - k_2 L_h^e \tag{19}$$

Make S_h^e a subject of the formula to get

$$S_h^e = \frac{Q_1 L_h^e + Q_2}{\mu k_1 k_3 k_4} \tag{20}$$

where

$$\left.\begin{aligned} Q_1 &= \rho\theta\gamma\sigma\mu + \delta\sigma k_4 - \mu k_2 k_3 k_4, \\ Q_2 &= \Lambda\mu k_3 k_4 - \Lambda k_3 k_4. \end{aligned}\right\} \tag{21}$$

Substitute equation (20) into the third equation of system (2) to get

$$\left[\beta_{HH} I_h^e + \frac{\beta_{EH} V_c^e}{K + V_c^e}\right]\left[\frac{Q_1 L_h^e + Q_2}{\mu k_1 k_3 k_4}\right] - k_2 L_h^e = 0.$$

Using equation (18) and solving explicitly gives

$$Q_3 L_h^{e2} + Q_4 L_h^e + Q_5, \text{ where,} \tag{22}$$

$$\left.\begin{aligned} Q_3 &= \beta_{HH}\sigma^2\pi Q_1, \\ Q_4 &= \beta_{HH}\sigma K k_3 k_5 Q_1 + \beta_{EH}\pi\sigma k_3 Q_1 + \beta_{HH}\sigma^2\pi Q_2 - k_2 k_3^2 k_1 \mu\pi\sigma k_4, \\ Q_5 &= \beta_{HH}\sigma K k_2 k_5 Q_2 + \beta_{EH}\pi\sigma k_3 Q_2 - k_2 K k_3^3 k_1 k_4 k_5 \mu, \end{aligned}\right\} \tag{23}$$

From the quadratic equation (22), we investigate the likelihood of multiple equilibrium states. It is imperative to note that the coefficient of Q_3 is always positive with Q_4 and Q_5 having different signs. The possible number of real roots is itemised in Table 3 using the Descarte's rule of signs [36].

Table 3: Existence of positive endemic states

Case	Q_3	Q_4	Q_5	Number of possible real roots	Range of R_0
1.	+	+	+	0	$R_0 < 1$
2.	+	+	-	1	$R_0 > 1$
3.	+	-	+	2	$R_0 < 1$
4.	+	-	-	1	$R_0 > 1$

From Table 3, it is evident that when $R_0 > 1$, the system admits a unique positive endemic equilibrium. Conversely, for $R_0 < 1$, there may exist either no endemic equilibrium or two endemic equilibria coexisting with the disease-free equilibrium E_0, thereby giving rise to a backward bifurcation at $R_0 = 1$.

3.4.1 Bifurcation analysis

The occurrence of either a backward or forward bifurcation is fundamental in assessing the stability of the endemic equilibrium, E^e. Specifically, when R_0 crosses the critical threshold of 1 such that the disease-free equilibrium becomes unstable and a stable endemic equilibrium emerges, the system undergoes a forward bifurcation [37]. A backward bifurcation means the model can have more than one stable outcome, even when $R_0 < 1$. This suggests that the norovirus may still persist under certain conditions, showing complex behaviour despite the reproduction number being below the usual threshold for disease elimination [14]. We analyse the model's bifurcation at $R_0 = 1$ by applying the Centre Manifold theorem developed by Castillo-Chavez and Song [38] with

$$a = \sum_{k,i,j=1}^{n} m_k w_i w_j \frac{\partial^2 q_k(E_0)}{\partial x_i \partial x_j} \text{ and } b = \sum_{k,i=1}^{n} m_k w_i \frac{\partial^2 q_k(E_0)}{\partial x_i \partial \varrho}$$

as bifurcation coefficients and ϱ as bifurcation parameter. Here, we consider the progression rate from the latent class to the infected class, $\sigma = \hat{\sigma}$ as the bifurcation parameter for the basic reproduction number, $R_0 = 1$. Since $R_0 = 1$, then

$$\hat{\sigma} = \frac{k_1 k_2 k_3 k_5 K}{\Lambda(\beta_{HH} k_5 K + \pi\beta_{EH})}.$$

Note that for $R_0 = 1$, the Jacobian matrix of the system equations, (2), has negative eigenvalues. Thus solving for a and b we obtain the left and right eigenvectors $m_k s$ and $w_i s$ respectively where $m = (m_1,\ m_2,\ m_3,\ m_4,\ m_5,\ m_6)$ and $w = (w_1,\ w_2,\ w_3,\ w_4,\ w_5,\ w_6)$ and $m \cdot w = 1$. Let

$$x_1 = S_h,\ x_2 = P_h,\ x_3 = L_h,\ x_4 = I_h,\ x_5 = R_h,\ x_6 = V_c, \tag{24}$$

and $q_1, q_2, q_3, q_4, q_5, q_6$ be the right hand sides of the system of equations (2). Therefore the non-zero second order partial derivatives of $q_1, q_2, q_3, q_4, q_5, q_6$ at disease-free equilibrium state, E_0 results in

$$\left.\begin{aligned} \frac{\partial^2 q_1(E_0)}{\partial x_1 \partial x_4} &= \frac{\partial^2 q_1(E_0)}{\partial x_4 \partial x_1} = -\beta_{HH},\ \frac{\partial^2 q_1(E_0)}{\partial x_1 \partial x_6} = \frac{\partial^2 q_1(E_0)}{\partial x_6 \partial x_1} = -\frac{\beta_{EH}}{K}, \\ \frac{\partial^2 q_3(E_0)}{\partial x_1 \partial x_4} &= \frac{\partial^2 q_3(E_0)}{\partial x_4 \partial x_1} = \beta_{HH},\ \frac{\partial^2 q_3(E_0)}{\partial x_1 \partial x_6} = \frac{\partial^2 q_3(E_0)}{\partial x_6 \partial x_1} = \frac{\beta_{EH}}{K}, \end{aligned}\right\} \tag{25}$$

and

$$\frac{\partial^2 q_3(E_0)}{\partial x_3 \partial \hat{\sigma}} = \frac{\partial^2 q_3(E_0)}{\partial \hat{\sigma} \partial x_3} = -1, \ \frac{\partial^2 q_4(E_0)}{\partial x_3 \partial \hat{\sigma}} = \frac{\partial^2 q_4(E_0)}{\partial \hat{\sigma} \partial x_3} = 1 \tag{26}$$

We obtain $m_k s$ and $w_i s$ as follows:

$$\begin{pmatrix} -k_1 & 0 & 0 & -\frac{\beta_{HH}\Lambda}{k_1} & \rho\theta & -\frac{\beta_{EH}\Lambda}{Kk_1} \\ \alpha & -\mu & 0 & 0 & (1-\rho)\theta & 0 \\ 0 & 0 & -k_2 & \frac{\beta_{HH}\Lambda}{k_1} & 0 & \frac{\beta_{EH}\Lambda}{Kk_1} \\ 0 & 0 & \sigma & -k_3 & 0 & 0 \\ 0 & 0 & 0 & \gamma & -k_4 & 0 \\ 0 & 0 & 0 & \pi & 0 & -k_5 \end{pmatrix} \begin{pmatrix} w_1 \\ w_2 \\ w_3 \\ w_4 \\ w_5 \\ w_6 \end{pmatrix} = \begin{pmatrix} 0 \\ 0 \\ 0 \\ 0 \\ 0 \\ 0 \end{pmatrix}.$$

Thus,

$$\left.\begin{aligned} -k_1 w_1 - \frac{\beta_{HH}\Lambda w_4}{k_1} + \rho\theta w_5 - \frac{\beta_{EH}\Lambda w_6}{Kk_1} = 0, \\ \alpha w_1 - \mu w_2 + (1-\rho)\theta w_5 = 0, \\ -k_2 w_3 + \frac{\beta_{HH}\Lambda w_4}{k_1} + \frac{\beta_{EH}\Lambda w_6}{Kk_1} = 0, \\ \hat{\sigma} w_3 - k_3 w_4 = 0, \\ \gamma w_4 - k_4 w_5 = 0, \\ \pi w_4 - k_5 w_6 = 0. \end{aligned}\right\} \tag{27}$$

It follows that

$$\left.\begin{aligned} w_1 = \frac{\rho\theta\gamma\hat{\sigma} w_3}{k_1 k_3 k_4} - \frac{\Lambda\sigma w_3}{k_1^2 k_3}\left[\beta_{HH} + \frac{\beta_{EH}\pi}{Kk_5}\right], \\ w_2 = \frac{\alpha}{\mu}\left[\frac{\rho\theta\gamma\hat{\sigma} w_3}{k_1 k_3 k_4} - \frac{\Lambda\sigma w_3}{k_1^2 k_3}\left[\beta_{HH} + \frac{\beta_{EH}\pi}{Kk_5}\right]\right] + \frac{(1-\rho)\theta\gamma\hat{\sigma} w_3}{\mu k_3 k_4}, \\ w_3 = w_3 > 0, \ w_4 = \frac{\hat{\sigma} w_3}{k_3}, \ w_5 = \frac{\gamma\hat{\sigma} w_3}{k_3 k_4}, \ w_6 = \frac{\pi\hat{\sigma} w_3}{k_3 k_5}. \end{aligned}\right\} \tag{28}$$

Also,

$$\begin{pmatrix} -k_1 & \alpha & 0 & 0 & 0 & 0 \\ 0 & -\mu & 0 & 0 & 0 & 0 \\ 0 & 0 & -k_2 & \hat{\sigma} & 0 & 0 \\ -\frac{\beta_{HH}\Lambda}{k_1} & 0 & \frac{\beta_{HH}\Lambda}{k_1} & -k_3 & \gamma & \pi \\ \rho\theta & (1-\rho)\theta & 0 & 0 & -k_4 & 0 \\ -\frac{\beta_{EH}\Lambda}{Kk_1} & 0 & \frac{\beta_{EH}\Lambda}{Kk_1} & 0 & 0 & -k_5 \end{pmatrix} \begin{pmatrix} m_1 \\ m_2 \\ m_3 \\ m_4 \\ m_5 \\ m_6 \end{pmatrix} = \begin{pmatrix} 0 \\ 0 \\ 0 \\ 0 \\ 0 \\ 0 \end{pmatrix}.$$

Hence,

$$\left.\begin{aligned} -k_1 m_1 + \alpha m_2 = 0, \\ -\mu m_2 = 0, \\ -k_2 m_3 + \hat{\sigma} m_4 = 0, \\ -\frac{\beta_{HH}\Lambda m_1}{k_1} + \frac{\beta_{HH}\Lambda m_3}{k_1} - k_3 m_4 + \gamma m_5 + \pi m_6 = 0, \\ \rho\theta m_1 + (1-\rho)\theta m_2 - k_4 m_5 = 0, \\ -\frac{\beta_{EH}\Lambda m_1}{Kk_1} + \frac{\beta_{EH}\Lambda m_3}{Kk_1} - k_5 m_6 = 0. \end{aligned}\right\} \tag{29}$$

This gives

$$\left.\begin{aligned} m_1 = m_2 = m_5 = 0, \ m_3 = m_3 > 0, \\ m_4 = \frac{\Lambda m_3}{k_1 k_3}\left(\beta_{HH} + \frac{\beta_{EH}\pi}{Kk_5}\right), \ m_6 = \frac{\beta_{EH}\Lambda m_3}{Kk_1 k_5}. \end{aligned}\right\} \tag{30}$$

We obtain a and b from equations (25), (26), (28) and (30). That is,

$$\left.\begin{aligned} a &= m_3 w_1 w_4 \frac{\partial^2 q_3(E_0)}{\partial x_1 \partial x_4} + m_3 w_1 w_6 \frac{\partial^2 q_3(E_0))}{\partial x_1 \partial x_6} \text{ and} \\ b &= m_3 w_3 \frac{\partial^2 q_3(E_0)}{\partial x_3 \partial \hat{\sigma}} + m_4 w_3 \frac{\partial^2 q_4(E_0)}{\partial x_3 \partial \hat{\sigma}}. \end{aligned}\right\} \tag{31}$$

So that,

$$a = \frac{m_3 w_3^2 \hat{\sigma^2}}{k_1 k_3^2}\left(1 + \frac{\pi}{k_5}\right)\left[\frac{\rho\theta\gamma}{k_4} - \frac{\pi}{k_1}\left(\beta_{HH} + \frac{\beta_{EH}\pi}{Kk_5}\right)\right].$$

Observe that $a < 0$ for $\frac{\rho\theta\gamma}{k_4} \leq \frac{\pi}{k_1}\left(\beta_{HH} + \frac{\beta_{EH}\pi}{Kk_5}\right)$ and $a > 0$ provided $\frac{\rho\theta\gamma}{k_4} > \frac{\pi}{k_1}\left(\beta_{HH} + \frac{\beta_{EH}\pi}{Kk_5}\right)$.

Additionally,

$$b = w_3 m_3 \Big[\frac{\Lambda}{k_1 k_3}\left(\beta_{HH} + \frac{\beta_{EH}\pi}{Kk_5}\right) - 1\Big].$$

So that, $b < 0$ if $\frac{\Lambda}{k_1 k_3}\left(\beta_{HH} + \frac{\beta_{EH}\pi}{Kk_5}\right) < 1$ while $b > 0$ if $\frac{\Lambda}{k_1 k_3}\left(\beta_{HH} + \frac{\beta_{EH}\pi}{Kk_5}\right) > 1$.

There exist a forward bifurcation for $a < 0$ and $b > 0$. The existence of a forward bifurcation implies that the requirement $R_0 < 1$ is necessary and sufficient for the elimination of the disease [37]. Consequently, there exist a backward bifurcation if $a > 0$ and $b > 0$. The presence of a backward bifurcation is as a result of reinfection where the disease-free equilibrium coexist with a stable endemic equilibrium for $R_0 < 1$ implying that a reduction of the basic reproduction number below unity may not be sufficient to eliminate the disease because small changes in model parameters can produce complicated changes in the equilibrium dynamics [25].

3.4.2 Global stability of the endemic equilibrium state

We examine the global stability of the endemic equilibrium E^e, to determine whether the system converges to this state for all valid initial conditions within the feasible region. We would state and proof the following theorem to establish the global stability of the endemic equilibrium state.

Theorem 3.5. *For $R_0 > 1$, the endemic equilibrium state, E^e, is globally asymptotically stable.*

Proof. Let

$$X = (S_h,\ P_h,\ L_h,\ I_h,\ R_h, V_c)^T.$$

Consider the Lyapunov function

$$\left.\begin{aligned} V(X) = &\Big[S_h - S_h^e - S_h \ln\frac{S_h}{S_h^e}\Big] + \Big[P_h - P_h^e - P_h \ln\frac{P_h}{P_h^e}\Big] \\ &+ a_1\Big[L_h - L_h^e - L_h \ln\frac{L_h}{L_h^e}\Big] + a_2\Big[I_h - I_h^e - I_h \ln\frac{I_h}{I_h^e}\Big] \\ &a_3\Big[R_h - R_h^e - R_h \ln\frac{R_h}{R_h^e}\Big] + a_4\Big[V_c - V_c^e - V_c \ln\frac{V_c}{V_c^e}\Big]. \end{aligned}\right\} \tag{32}$$

Computing equation (32) explicitly gives

$$\left.\begin{aligned} V' = &\Big[1 - \frac{S_h^e}{S_h}\Big]S_h' + \Big[1 - \frac{P_h^e}{P_h}\Big]P_h' + a_1\Big[1 - \frac{L_h^e}{L_h}\Big]L_h' \\ &+ a_2\Big[1 - \frac{I_h^e}{I_h}\Big]I_h' + a_3\Big[1 - \frac{R_h^e}{R_h}\Big]R_h' + a_4\Big[1 - \frac{V_c^e}{V_c}\Big]V_c'. \end{aligned}\right\} \tag{33}$$

By employing the system of equations (2), equation (33) becomes

$$\left.\begin{aligned} V' = &\Big[1-\frac{S_h^e}{S_h}\Big]\Big[\Lambda-\Big(\beta_{HH}I_h+\frac{\beta_{EH}V_c}{K+V_c}\Big)S_h+\rho\theta R_h-(\alpha+\mu)S_h\Big]\\ &+\Big[1-\frac{P_h^e}{P_h}\Big]\Big[\alpha S_h+(1-\rho)\theta R_h-\mu P_h\Big]\\ &+a_1\Big[1-\frac{L_h^e}{L_h}\Big]\Big[\Big(\beta_{HH}I_h+\frac{\beta_{EH}V_c}{K+V_c}\Big)S_h-k_2L_h\Big]\\ &+a_2\Big[1-\frac{I_h^e}{I_h}\Big]\Big[\sigma L_h-k_3I_h\Big]+a_3\Big[1-\frac{R_h^e}{R_h}\Big]\Big[\gamma I_h-k_4R_h\Big]\\ &+a_4\Big[1-\frac{V_c^e}{V_c}\Big[\pi I_h-k_5V_c\Big], \end{aligned}\right\} \tag{34}$$

where $a_1,\ a_2,\ a_3,\ a_4$ are unknown constants. At endemic equilibrium state, we have

$$\left.\begin{aligned} &\Lambda=\Big(\beta_{HH}I_h^e+\frac{\beta_{EH}V_c^e}{K+V_c^e}\Big)S_h^e-\rho\theta R_h^e+(\alpha+\mu)S_h^e,\ k_2=\Big(\beta_{HH}I_h^e+\frac{\beta_{EH}V_c^e}{K+V_c^e}\Big)\frac{S_h^e}{L_h^e},\\ &k_3=\frac{\sigma L_h^e}{I_h^e},\ k_4=\frac{\gamma I_h^e}{R_h^e},\ k_5=\frac{\pi I_h^e}{V_c^e}. \end{aligned}\right\} \tag{35}$$

Using equation (35), equation (34) becomes

$$\left.\begin{aligned} V' = &\Big[1-\frac{S_h^e}{S_h}\Big]\Big[\Big(\beta_{HH}I_h^e+\frac{\beta_{EH}V_c^e}{K+V_c^e}\Big)S_h^e-\rho\theta R_h^e+(\alpha+\mu)S_h^e-\Big(\beta_{HH}I_h+\frac{\beta_{EH}V_c}{K+V_c}\Big)S_h\\ &+\rho\theta R_h-(\alpha+\mu)S_h\Big]+\Big[1-\frac{P_h^e}{P_h}\Big]\Big[\alpha S_h+(1-\rho)\theta R_h-\mu P_h-\alpha S_h^e-(1-\rho)\theta R_h^e+\mu P_h^e\Big]\\ &+a_1\Big[1-\frac{L_h^e}{L_h}\Big]\Big[\Big(\beta_{HH}I_h+\frac{\beta_{EH}V_c}{K+V_c}\Big)S_h-\Big(\beta_{HH}I_h^e+\frac{\beta_{EH}V_c^e}{K+V_c^e}\Big)\frac{S_h^e}{L_h^e}L_h\\ &-\Big(\beta_{HH}I_h^e+\frac{\beta_{EH}V_c^e}{K+V_c^e}\Big)S_h^e+\Big(\beta_{HH}I_h^e+\frac{\beta_{EH}V_c^e}{K+V_c^e}\Big)\frac{S_h^e}{L_h^e}L_h^e\Big]+a_2\Big[1-\frac{I_h^e}{I_h}\Big]\\ &\Big[\sigma L_h-\frac{\sigma L_h^e}{I_h^e}I_h-\sigma L_h^e+\frac{\sigma L_h^e}{I_h^e}I_h^e\Big]+a_3\Big[1-\frac{R_h^e}{R_h}\Big]\Big[\gamma I_h-\frac{\gamma I_h^e}{R_h^e}R_h-\gamma I_h^e+\frac{\gamma I_h^e}{R_h^e}R_h^e\Big]\\ &+a_4\Big[1-\frac{V_c^e}{V_c}\Big]\Big[\pi I_h-\frac{\pi I_h^e}{V_c^e}V_c-\pi I_h^e+\frac{\pi I_h^e}{V_c^e}V_c^e\Big]. \end{aligned}\right\} \tag{36}$$

Let

$$\frac{S_h}{S_h^e}=n_1,\ \frac{P_h}{P_h^e}=n_2,\ \frac{L_h}{L_h^e}=n_3,\ \frac{I_h}{I_h^e}=n_4,\ \frac{R_h}{R_h^e}=n_5,\ \frac{V_c}{V_c^e}=n_6.$$

Solving equation (36) explicitly, we obtain $a_1=a_2=a_4=0,\ a_3=\theta R_h^e$ and equation (36) becomes

$$\left.\begin{aligned} V' = &-\Big[\mu\frac{(1-n_1)^2}{n_1}+\mu\frac{(1-n_2)^2}{n_2}\Big]+\rho\theta R_h^e\left[\frac{1}{n_1}+n_5-\frac{n_5}{n_1}-1\right]\\ &+\alpha S_h^e\left[1+\frac{1}{n_2}-\frac{1}{n_1}-\frac{n_1}{n_2}\right]+(1-\rho)\theta R_h^e\left[n_5+\frac{1}{n_2}-\frac{n_5}{n_2}-1\right]\\ &+\theta R_h^e\left[1+n_4-n_5-\frac{n_4}{n_5}\right]. \end{aligned}\right\} \tag{37}$$

Consider the function $v(x)=1-x+\ln(x)$, which satisfies $v(x)\le 0$ for all $x>0$, with equality attained only at $x=1$. Given that $1-x\le-\ln(x)$, it follows that the term $\rho\theta R_h^e$ transforms into

$$\left(1-\frac{n_5}{n_4}\right)-(1-n_5)-\left(1-\frac{1}{n_1}\right)\le-\ln\frac{n_5}{n_1}+\ln n_5+\ln\frac{1}{n_1}=\ln\left(\frac{n_1}{n_5}\cdot n_5\cdot\frac{1}{n_1}\right)=0.$$

Similarly, the $\alpha S_h^e,\ (1-\rho)\theta R_h^e$ and θR_h^e terms becomes

$$\left(1-\frac{1}{n_1}\right)-\left(1-\frac{1}{n_2}\right)+\left(1-\frac{n_1}{n_2}\right)\leq -\ln\frac{1}{n_1}+\ln\frac{1}{n_2}-\ln\frac{n_1}{n_2}=\ln\left(n_1\cdot\frac{1}{n_2}\cdot\frac{n_2}{n_1}\right)=0,$$

$$\left(1-\frac{n_5}{n_2}\right)-\left(1-\frac{1}{n_1}\right)-(1-n_5)\leq -\ln\frac{n_5}{n_2}+\ln\frac{1}{n_2}+\ln n_5=\ln\left(\frac{n_2}{n_5}\cdot\frac{1}{n_2}\cdot n_5\right)=0,$$

$$(1+n_4)-(1+n_5)+\left(1-\frac{n_4}{n_5}\right)\leq \ln n_4-\ln n_5-\ln\frac{n_4}{n_5}=\ln\left(n_4\cdot\frac{1}{n_5}\cdot\frac{n_5}{n_4}\right)=0.$$

It follows that

$$V'=-\mu\Big[\frac{(1-n_1)^2}{n_1}+\frac{(1-n_2)^2}{n_2}\Big]\leq 0.$$

By LaSalle's invariance principle [39], it follows that for $R_0>1$, as $t\longrightarrow\infty$, the endemic equilibrium state is globally asymptotically stable.

This implies that norovirus would remain in the population if $R_0>1$ irrespective of the number of infected humans in the population. Even if there is a decline in the rate of infection, the norovirus will remain in the population making its eradication quite challenging.

3.5 Sensitivity Analysis

In this subsection, we conducted a global sensitivity analysis using the Partial Rank Correlation Coefficient (PRCC) method with Latin Hypercube Sampling (LHS) to assess the significance of each parameter in the transmission dynamics of norovirus, based on 1000 runs as adopted by [13, 40], and employing the parameter values in Table 2. The graphical presentation of PRCCs for the parameters affecting R_0 is shown in Figure 2. Parameters with positive values increase the reproduction number, thereby facilitating disease spread. Conversely, parameters with negative values decrease the reproduction number as their magnitude increases, thereby reducing disease transmission within the population. Hence, in Figure 2, as disease induced death rate, δ, pathogen decay due to disinfection and proper sanitation, μ_a, pathogen natural deacy, μ_v, recovery rate due to screening and supportive treatment, γ and the progress rate from S_h to P_h, α increase, the reproduction number reduces, leading to the reduction of the disease in the society. On the other hand, as the shedding rate, π, progress rate from L_h to I_h, σ, effective transmission rate from environment-to-human, β_{EH} and effective transmission rate from human-to-human, β_{HH} increase, the reproduction number increases and this results in the increase in the spread of the disease in the community. Meanwhile, it is noteworthy to mention that the parameters with PRCCs values ≥ 0.5 are more significant in influencing the transmission dynamics of the norovirus. Hence, μ_a, γ, π and β_{EH} are more significant in influencing the spread of the norovirus in the population.
Also, Figure 3 is the $3D$ plot showing the effects of of environment-to-human transmission, β_{EH} and the bacteria decay μ_a on R_0. It can be observed that as the bacteria decay μ_a increases, the R_0 decreases while as β_{EH} the R_0 increases and then, the disease spread increases.

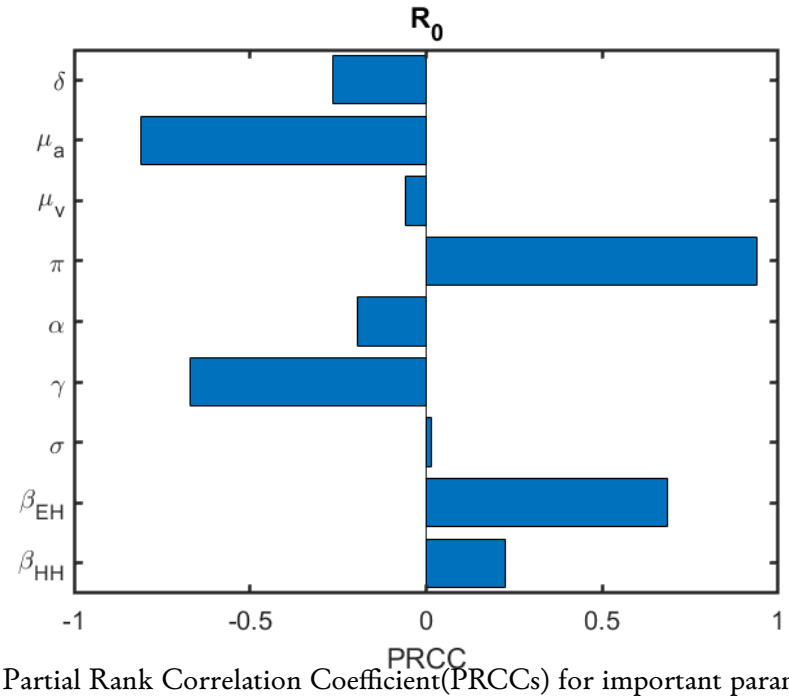

Figure 2: Partial Rank Correlation Coefficient(PRCCs) for important parameters of R_0.

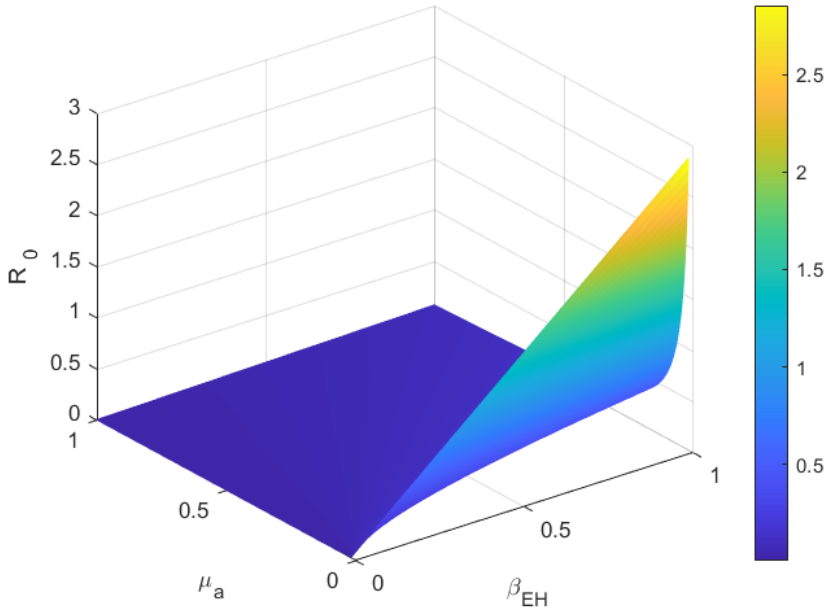

Figure 3: 3D plot showing the impact of environment-to-human transmission, β_{EH} and the bacteria decay μ_a on R_0.

4 Numerical Simulations

Here, numerical simulations are performed using the fourth-order Runge–Kutta method implemented in MATLAB R2024a. The parameter values employed in the simulations are provided in Table 1, and the initial conditions are as follows: $S_h(0) = 1{,}000{,}000,\ P_h(0) = 50{,}000,\ L_h(0) = 50,\ I_h(0) = 20,\ R_h(0) = 5,\ V_c(0) = 20$. The numerical simulations are implemented to illustrate the impacts of the effective transmission rate from environment to human, β_{EH}, the effective transmission rate from human to human, β_{HH}, the recovery rate due to screening and supportive treatment, γ, the progression

rate from L_h to I_h, σ, pathogen decay due to disinfection and proper sanitation, μ_a, and the shedding rate, π, on the infected population.

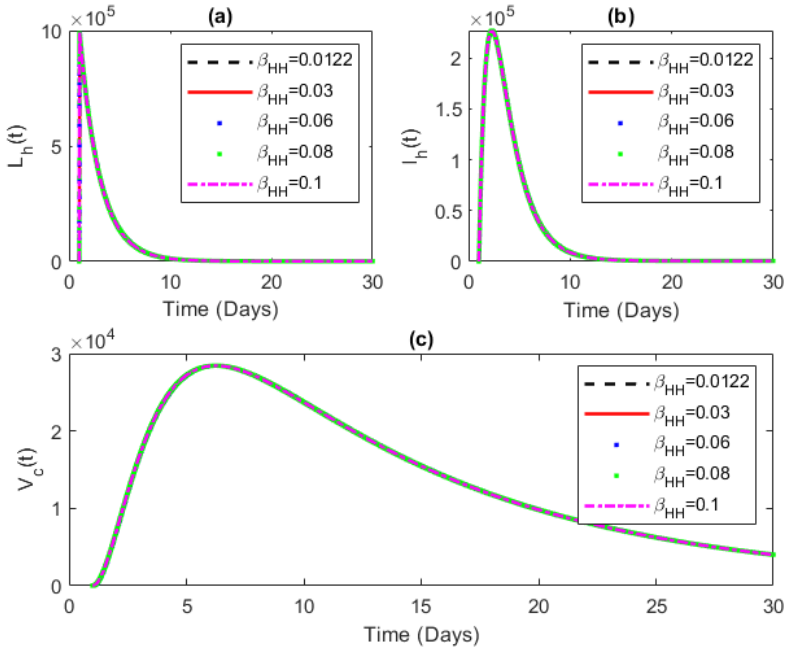

Figure 4: Impact of human-to-human transmission rate, β_{HH} on the disease spread.

Figure 4 illustrates the impact of the effective transmission rate from human-to-human, β_{EH}, on $L_h, I_h,$ and V_c. The infection peaks in L_h and I_h around days 2–3 and then declines rapidly to nearly zero, reflecting the fact that norovirus spreads quickly and has a short incubation and recovery period. In contrast, the V_c compartment continues to increase, reaching a minimum of about 5,000 at day 50, since the virus persists much longer in the environment as infected individuals continue to shed it. Therefore, to curb the disease in society, effective disinfection, proper sanitation, and good hygiene practices must be maintained, as recommended by [1]. Similarly, the impact of the effective environment to human transmission rate, β_{HH}, which have the same effect on $L_h, I_h,$ and V_c is shown in Figure 5.

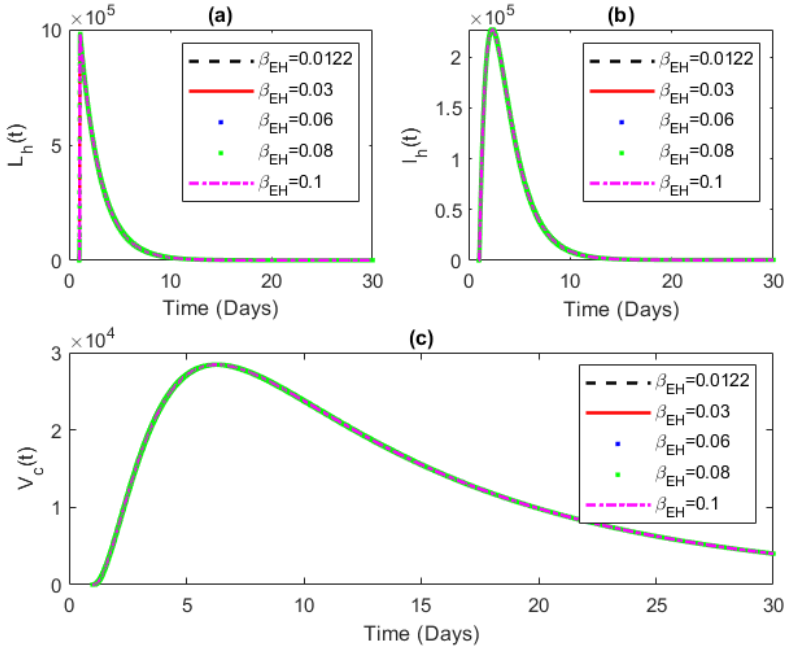

Figure 5: Impact of environment-to-human transmission rate, β_{EH} on the disease spread.

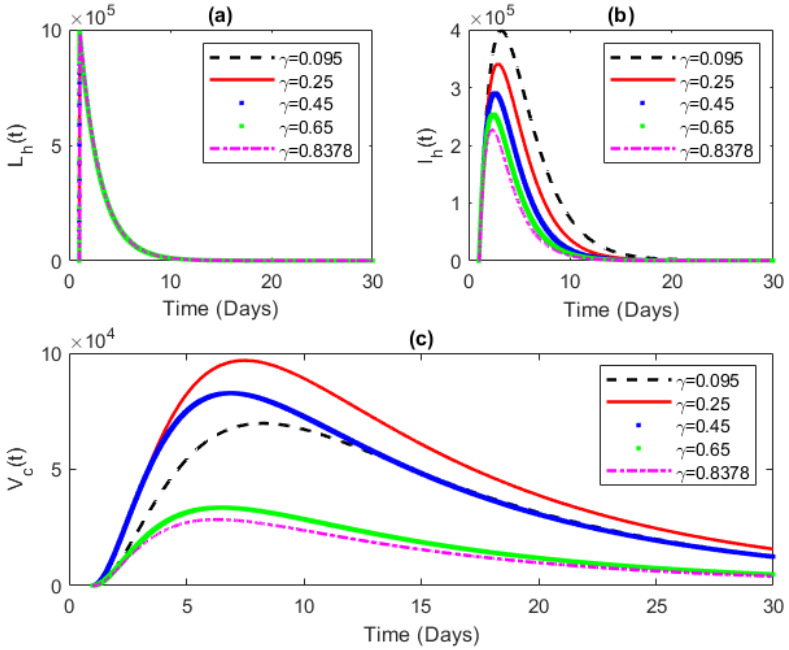

Figure 6: Impact of human recovery rate, γ on the disease spread.

Figure 6 illustrates the effects of the recovery rate due to screening and supportive treatment, γ, on the pre-infectious (L_h), infected (I_h), and pathogen (V_c) populations. The results show that as screening and supportive treatment increase, both the number of infected individuals and the pathogen concentration in the environment decrease. Therefore, to control the spread of the disease, effective screening and supportive treatment must be implemented, including measures to prevent viral shedding into the environment. This is consistent with the recommendations of [6].

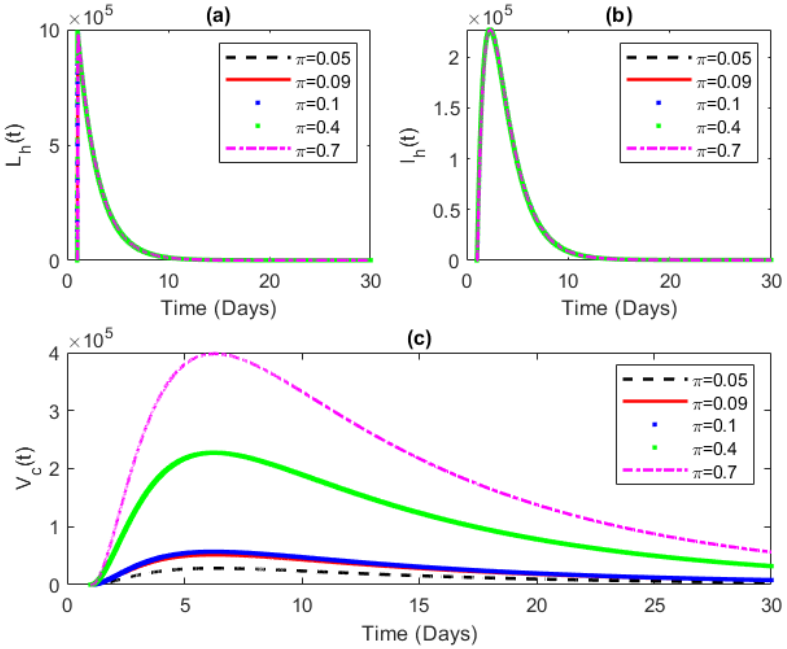

Figure 7: Impact of shedding rate, π on the disease spread.

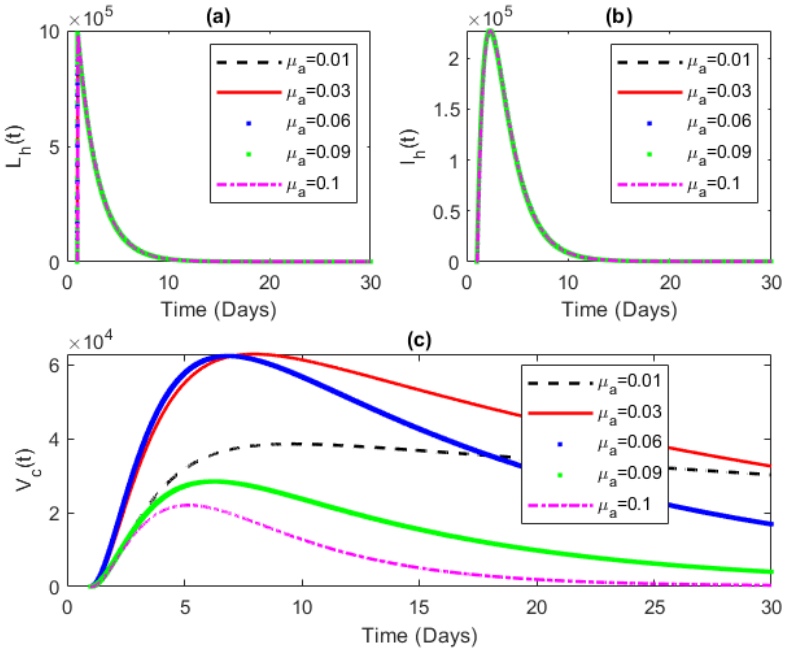

Figure 8: Impact of virus decay rate, μ_a due to disinfection and proper sanitation on the disease spread.

Figures 7 and 8 illustrate the impact of the shedding rate, π, and the virus decay rate, μ_a, due to disinfection and proper sanitation, on the infected human population and the contaminated environment. As the shedding rate π increases, the spread of the disease also increases. Conversely, as the virus decay rate μ_a rises through effective disinfection and sanitation, environmental contamination with norovirus decreases, thereby reducing the risk of transmission from environment to human, as noted by [1].

5 Conclusion

This paper examines the role of environmental contamination, screening, and supportive treatment in the transmission dynamics of norovirus through the formulation of a nonlinear deterministic mathe-

matical model with six compartments. The basic reproduction number, R_0, which serves as a critical threshold for assessing norovirus dynamics, is calculated, and the stability of both the disease-free and endemic equilibrium states is established. Findings from the global sensitivity analysis indicate that the pathogen decay rate due to disinfection and proper sanitation (μ_a), the recovery rate associated with screening and supportive treatment (γ), the shedding rate of infected individuals into the environment (π), and the effective environment-to-human transmission rate are key parameters influencing disease spread, with π identified as the most dominant factor.

Numerical simulations suggest that effective control of norovirus in society requires the implementation of intensive screening and supportive treatment, along with good hygiene practices, disinfection, and proper sanitation, in line with the recommendations of Towers *et al.* [24].

This study has limitations, including reliance on assumed parameter values or values drawn from the literature, as well as failure to account for the influence of climatic factors such as humidity, temperature, rainfall, and extreme weather events, all of which affect norovirus persistence and transmission and pose a growing concern for its control and public health. Furthermore, optimal control analysis and cost-effectiveness evaluation of the proposed strategies, essential for ensuring efficient use of limited resources and identifying the most cost-effective intervention, were not addressed. These aspects will be considered in future research.

References

[1] Centre for Disease Control (CDC), https://www.cdc.gov/norovirus/about/index.html, last accessed 2025/09/29.

[2] World Health Organisation (WHO), https://www.who.int/teams/immunization-vaccines-and-biologicals/diseases/norovirus, last accessed 2025/09/29.

[3] Winder, N., Gohar, S. and Muthana, M. (2022). Norovirus: an overview of virology and preventative measures. Viruses 14(12), 2811.

[4] Capece, G. and Tobin, E. H. (2025). Norovirus, [Updated 2025 Feb 17]. In: StatPearls [Internet]. Treasure Island (FL): StatPearls Publishing;https://www.ncbi.nlm.nih.gov/books/NBK513265/

[5] Centre for Disease Control (CDC), https://www.cdc.gov/yellow-book/hcp/travel-associated-infections-diseases/norovirus.html, last accessed 2025/09/29.

[6] Centre for Health Protection | The Government of the Hong Kong Special Administrative Region | Department of Health. Norovirus Infection, (2025). https://www.chp.gov.hk/en/healthtopics/content/24/33.html.

[7] National Health and Medical Research Council (NHMRC). (2024)https://www.nhmrc.gov.au/about-us/publications/staying-healthy-guidelines/fact-sheets/norovirus-infection, last accessed 2025/09/29.

[8] Mathscareers. (2021). https://www.mathscareers.org.uk/what-is-mathematical-modelling/ , last accessed 2025/09/29.

[9] Tilahum, G. T., Oluwole, D. M. and David, M. (2017). Modelling and optimal control of typhoid fever disease with cost effective strategies, Computational and Mathematical Methods in Medicine, 2324518, https://doi.org/10.1155/2017.

[10] Zaman, G., Jung, I. H., Torres, F. M. D. and Zeb, A. (2017). Mathematical modelling and control of infectious disease, Computational and Mathematical Method in Medicine, 7149154, https://doi.org/10.1155/2017/7149154.

[11] Madubueze, C. E., Gweryina, R. I. and Abokwara, A. (2022). Mathematical analysis and optimal control of schistosomiasis transmission model. Biomath Communications 9(8), 2203071-2203071 .

[12] Madubueze, C. E., Tijani, K. A. and Fatmawati. (2023). A deterministic mathematical model for optimal control of diphtheria disease with booster vaccination. Healthcare Analytics 4,100281.

[13] Tijani, K . A, Madubueze, C.E, and Gweryina, R I. (2023). Typhoid fever dynamical model with cost-effective optimal control. Journal of the Nigerian Society of Physical Sciences 5(4), 1579. https://doi.org/10.46481/jnsps.2023.1579.

[14] Abokwara, A. and Madubueze C. E. (2025a). Optimal control analysis of lymphatic filariasis transmission dynamics. In: The Second International Conference on Mathematical Modelling Optimization and Analysis on Disease Dynamics 2025, 27-40.

[15] Sayooj, A. J., Karuna, M., Hamna, M. K. B., Jirawattana-panit, A. and Anurak, W. (2024). Analysing and forecasting dengue fever incidence in Thailand: a comprehensive study for public health preparedness. International Journal of Biomathematics, doi: 10.1142/S1793524524501328

[16] Gaythorpe, K. A. M., Trotter, C. L., Lopman, B., Steele, M., and amp; Conlan, A. J. K. (2017). Norovirus transmission dynamics: a modelling review. Epidemiology and Infection 146(2), https://doi.org/10.1017/s0950268817002692

[17] Gaythorpe, K. A. M., Trotter, C. L. and Conlan, A. J. K. (2018). Modelling norovirus transmission and vaccination. 36 (37), 5565-5571.

[18] Gogovi, G. K., Qin, L., String, G., and Olaniyi, S. (2024). Analysis of a compartmental model for norovirus transmission through environmental contact. International Journal of Differential Equations 1, 5517340. https://doi.org/10.1155/ijde/5517340

[19] Lopman, B., Simmons, K., Gambhir, M., Vinjé, J. and Parashar, U. (2013). Epidemiological implications of asymptomatic reinfection: A mathematical modelling study of norovirus. American Journal of Epidemiology, DOI: 10.1093/aje/kwt287.

[20] Song, Y., Liu, P., and Din, A. (2024). A Novel stochastic model for human norovirus dynamics: Vaccination impact with lévy noise. Fractal and Fractional 8(6), 349.

[21] Ting, C., Liu, P. and Din, A. (2021). Fractal–fractional and stochastic analysis of norovirus transmission epidemic model with vaccination. Scientific Reports, https://doi.org/10.1038/s41598-021-03732-8.

[22] Raezah, A. A., Zarin, R., and Raizah, Z. (2023). Numerical approach for solving a fractional-order norovirus epidemic model with vaccination and asymptomatic carriers. Symmetry, 15(6), 1208.

[23] Saleem, S., Raza, A., Lampart, M., Rafiq, M., Ahmed, N. and Arif, M. S. (2025). Numerical solutions for norovirus epidemic spread: implications for public health control. Scientific Reports 15, 29657 .

[24] Towers, S., Chen, J., Cruz, C., Melendez, J., Rodriguez, J., Salinas, A., Yu, F. and Kang, Y. (2018). Quantifying the relative effects of environmental and direct transmission of norovirus. Royal Society Open Science, http://doi.org/10.1098/rsos.170602.

[25] Abokwara, A. and Madubueze, C. E. (2025b). Optimizing the control of lymphatic filariasis: A mathematical modelling and cost effectiveness analysis. Discover Public Health 22(1),703 https://doi.org/10.1186/s12982-025-01058-8.

[26] Becker, N. G. and Glass, K. (1987). Estimating the population impact of a new gastrointestinal infection in the community. Epidemiology and Infection 99(3), 619-634.

[27] Tsang, T. K., Chen, T. M., Longini, I. M., Jr, Halloran, M. E., Wu, Y. and Yang, Y. (2018). Transmissibility of norovirus in urban versus rural households in a large community outbreak in China. Epidemiology (Cambridge, Mass.) 29(5), 675–683.

[28] Rwezaura, H. (2021). Modelling the impact of undetected cases on the transmission dynamics of COVID-19. Tanzania Journal of Science, 47(5), 1793-1809.

[29] Harrington, R. A. (2008). Case fatality rate. Accessed from https://www.britannica.com/science/case-fatality-rate

[30] Rexin, D., Rachmadi, A. T., and Hewitt J. (2024). Persistence of infectious human norovirus in estuarine water. Food and Environmental Virology 16(1), 58–64.

[31] Gosh, M., Chandra, P., Sinha, P. and Shukla, J. B. (2006). Modelling the spread of bacterial infectious disease with environmental effect in a logistically growing human population. Nonlinear - Analysis: Real World Applications 7,341–363

[32] Birkhoff, G. and C. Rota, C. (1998). Ordinary Differential Equation. 4th edn. John Wiley and Sons, New York,

[33] Ogunmodimu, M., Yusuf, T., and Olotu, O. (2025). Sensitivity and stability analyses of COVID-19 model with waning immunity and relapse: a case study of Nigeria. International Journal of Mathematical Analysis and Modelling 8(1).

[34] Tijani, K . A., Madubueze, C. E, and Gweryina, R. I. (2024). Modelling typhoid fever transmission with treatment relapse response: optimal control and cost-effectiveness analysis. Mathematical Models and Computer Simulations 16, 457–485.

[35] Castillo-Chavez, C. Feng, Z. and Huang, W. (2001). On the computation of R_0 and its role on the global stability. https://ecommons.cornell.edu/server/api/core/bitstreams/06bba96f-726c-4d38-bb18-3db9251e63a7/

[36] Jameson, G. (2006). Counting zeros of generalised polynomials: Descartes rule of signs and laguerres extensions. The Mathematical Gazette 90(518), 223-234.

[37] Gumel, A. B. (2012). Causes of backward bifurcations in some epidemiological models. Journal of Mathematical Analysis and Applications 395,355-365.

[38] Castillo-Chavez, C. Song, B. (2004). Dynamical models of tuberculosis and their applications, Mathematical Biosciences and Engineering 1(2), 361–404.

[39] LaSalle, J. and Lefschetz, S. (1976). The stability of dynamical systems. SIAM Philadelphia.

[40] Tijani, K. A. and Madubueze, C. E. (2025). Understanding the dynamics of ameobiasis using mathematical modelling approach: optimal control strategies and cost-effectiveness analysis. International Journal of Mathematical Sciences and Optimization: Theory and Applications 11(3), 138–166.